Appl. Magn. Reson. 11, 391–399 (1996)

Applied Magnetic Resonance

Line-Shifting Method in Electron Spin Echo Envelope Modulation (ESEEM) Studies

R. Song, Y. C. Zhong, C. J. Noble, J. R. Pilbrow, and D. R. Hutton

Department of Physics, Monash University, Clayton, Australia

Received November 21, 1995; revised February 21, 1996

Abstract. A novel line-shifting method, which is called mixing-frequency electron spin echo envelope modulation (MIF-ESEEM) spectroscopy, is introduced and analysed. It is shown that the spectral resolution is enhanced, and thus the overlapping is removed with this new method. The application of this method to systems with $S \geq 1$ and $I \geq 1$ is also discussed.

1. Introduction

Recent pulsed-EPR technological developments in electron spin echo envelope modulation (ESEEM) spectroscopy have led to its general acceptance as a powerful alternative to ENDOR spectroscopy for the determination of nuclear transition frequencies [1]. The ESEEM experiments are commonly performed either by using a two-pulse primary echo or a three-pulse simulated echo sequences [2]. The two-pulse primary echo sequence was improved by a five-pulse sequence to increase the modulation depth, by adding three refocusing pulses ($\pi/2 - \pi - \pi/2$) before the two original pulses [3]. The three-pulse stimulated echo sequence was developed into a four-pulse two-dimensional (2D) ESEEM experiment [4], named HYSCORE (hyperfine sublevel correlation) spectroscopy, by inserting a mixing π pulse between the second and third $\pi/2$ pulses. Recently the original four-pulse 2D ESEEM scheme has been improved with a six-pulse 2D ESEEM experiment to increase cross peaks and suppress diagonal peaks, by tucking in a mixing π pulse between the third and fourth pulses in the five-pulse sequence [5]. In all of those ESEEM experiments, the emphasis is on the basic nuclear transition frequencies ω_α and ω_β.

However, the assignment of peaks in those 1D or 2D ESEEM spectra is often complicated by overlapping. Although a number of attempts have been done to solve the overlapping problem [6], all of them are focused on the recovery of broad ESEEM lines by means of mathematical reconstruction or by elimination

of dead-time effects. Recently, a mixing-frequency ESEEM spectroscopy has been introduced [7, 8]. Instead of reducing the widths of overlapped lines, increasing the separation between the overlapped lines is realized to solve the overlapping problem. By choosing different increment ratios, the peaks in a spectrum can be shifted in a controlled manner. This provides a practical solution to the overlapping problem in ESEEM studies.

In this paper, further discussion of this new approach is presented. This method is compared with the conventional method under the condition which uses the same time range so as to illustrate its unique advantage and usefulness in relation to the enhancement of ESEEM spectral resolution. The application of this method to high spin systems are also discussed.

2. Theory

2.1. 1D Mixing-Frequency ESEEM (MIF-ESEEM) Spectroscopy

For the sake of simplicity, we focus ourself on the systems with weak hyperfine interactions (HFI). The 2D ESEEM formula, assuming ideal $\pi/2$ and π pulses, for the spin system of $S = 1/2$ and $I = 1/2$ can be written as [9]:

$$S(t_1, t_2) = A_c[\cos(\omega_\alpha t_1 + \omega_\beta t_2 + \phi_+) + \cos(\omega_\alpha t_2 + \omega_\beta t_1 + \phi_+)] \ . \qquad (1)$$

Only the terms which correspond to cross peaks are retained in Eq. (1), and the terms which correspond to strong HFI are also ignored. The amplitude A_c and phase factor ϕ_+ are independent of t_1 and t_2. Traditionally, in all the existing 2D-ESEEM experiments, the amplitude of the electron spin echo is monitored as a function of the two time variables, t_1 and t_2, so that two pairs of cross peaks at $(\omega_\alpha, \omega_\beta)$ and $(\omega_\beta, \omega_\alpha)$ symmetrical about the diagonal line $\omega_1 = \omega_2$, are detected. However, alternative approaches are possible for manipulating ESEEM spectra during detection of ESEEM signals as shown here. To achieve our goal of peak manipulation, the time intervals t_1 and t_2 are changed at different rates,

$$\begin{aligned} t_1 &= t_{10} + t \ , \\ t_2 &= t_{20} + \gamma t \ , \end{aligned} \qquad (2)$$

where the increment ratio $\gamma = \Delta t_2/\Delta t_1$ is a constant. Thus in our experiments, t_1 and t_2 are changed with increments $\Delta t_1 = \Delta t$ and $\Delta t_2 = \Delta(\gamma t)$, respectively. The initial times t_{10} and t_{20} are fixed, and are chosen to ensure that $t_1 > 0$ and $t_2 > 0$, whenever Δt_1 or Δt_2 is chosen to be a negative increment. Substituting Eq. (2) into Eq. (1), we obtain an alternative form in two variables

$$S(t, \gamma) = C_c c^2[\cos(\Omega_a t + \Phi_a) + \cos(\Omega_b t + \Phi_b)] \ , \qquad (3)$$

where

$$\Omega_a = \omega_\alpha + \gamma\omega_\beta \ , \qquad \Phi_a = \omega_\alpha t_{10} + \omega_\beta t_{20} + \phi_+ \ ,$$
$$\Omega_b = \gamma\omega_\alpha + \omega_\beta \ , \qquad \Phi_b = \omega_\alpha t_{20} + \omega_\beta t_{10} + \phi_+ \ . \tag{4}$$

Equations (3) and (4) show that the spectrum comprises the modulation frequencies Ω_a, Ω_b. It is clear that the values of the frequencies in this new spectrum are the admixtures of basic frequencies ω_α and ω_β. Hence, such a spectrum is called a 1D mixing-frequency ESEEM (MIF-ESEEM) spectrum to distinguish it from a conventional 1D ESEEM spectrum, which will be designated as 1D basic-frequency ESEEM (BF-ESEEM) spectrum in this study accordingly. Obviously, the BF-ESEEM spectroscopy is just a special case of MIF-ESEEM spectroscopy where $\gamma = 0$.

2.2. 2D Mixing-Frequency ESEEM (MIF-ESEEM) Spectroscopy

Naturally, the 1D MIF-ESEEM method can be developed into a 2D scheme. The two evolution times, t_1 and t_2, are further divided into two parts as follows (see Figs. 1a and 1b)

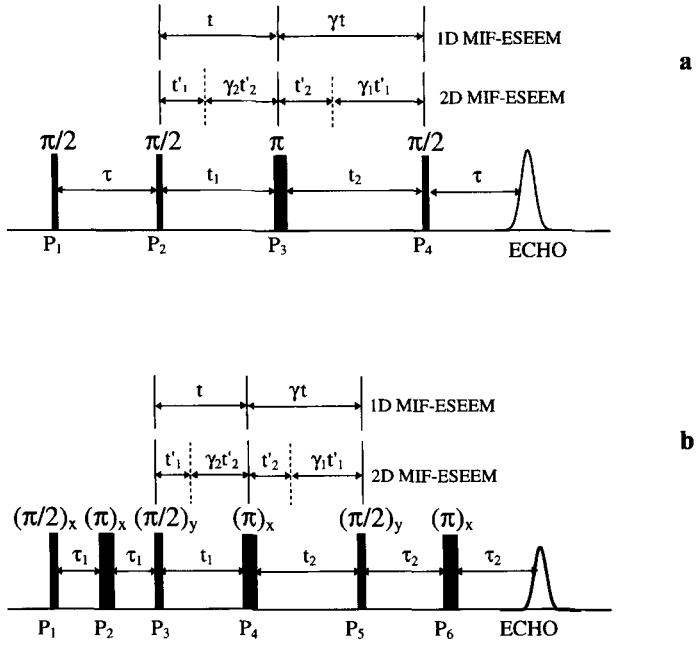

Fig. 1. The pulse sequences discussed in the text. A four-pulse sequence (**a**), a six-pulse scheme (**b**).

$$t_1 = t_{10} + t_1' + \gamma t_2' \ ,$$
$$t_2 = t_{20} + \gamma t_1' + t_2' \ , \tag{5}$$

where $\gamma = \Delta t_2/\Delta t_1$ while t_2' is kept constant, or $\gamma = \Delta t_1/\Delta t_2$ while t_1' is fixed, and Δt_1 and Δt_2 are the time increments of t_1 and t_2, respectively. t_{10} and t_{20} are initial values for t_1 and t_2, respectively, to ensure t_1 and t_2 are always greater than zero. To be more specific, in the experiments, $(1 + \gamma_1)t_1'$ is acquired as one dimension, and $(1 + \gamma_2)t_2'$ is used as the other. Substituting Eq. (5) into Eq. (1), we obtain

$$S(t_1, t_2) = A_c[\cos(\Omega_a t_1' + \Omega_b t_2' + \omega_\alpha t_{10} + \omega_\beta t_{20} + \phi_+) + \cos(\Omega_b t_1' + \Omega_a t_2' + \omega_\beta t_{10} + \omega_\alpha t_{20} + \phi_+)] \ , \tag{6}$$

where

$$\Omega_a = \omega_\alpha + \gamma\omega_\beta \ ,$$
$$\Omega_b = \gamma\omega_\alpha + \omega_\beta \ . \tag{7}$$

Equations (6) and (7) indicate that the pair of cross peaks at $[(\omega_\alpha, \omega_\beta), (\omega_\beta, \omega_\alpha)]$ are now in effect shifted to $[(\Omega_a, \Omega_b), (\Omega_b, \Omega_a)]$. To be consistent with our definitions of different ESEEM methods, this spectroscopy is called 2D mixing-frequency ESEEM (MIF-ESEEM) spectroscopy. Obviously, the 2D basic-frequency(BF)-ESEEM spectroscopy, in fact is a special case of MIF-ESEEM spectroscopy where $\gamma_1 = \gamma_2 = 0$.

2.3. Separation of Overlapped Peaks in an ESEEM Spectrum

As a result of position shifting of ESEEM spectra through changing γ, it is now possible to separate overlapped peaks. Consider two overlapped peaks at $\omega_{\alpha 1}$ and $\omega_{\alpha 2}$, the separation is

$$\Delta_0 = \omega_{\alpha 2} - \omega_{\alpha 1} = \Delta\omega_\alpha \tag{8}$$

in a conventional 1D BF-ESEEM spectrum. In a mixing-frequency ESEEM spectrum with increment ratio γ, this becomes

$$\Delta_\gamma = \Omega_{a2} - \Omega_{a1} = \Delta\omega_\alpha + \gamma\Delta\omega_\beta \ , \tag{9}$$

where $\Delta\omega_\alpha = \omega_{\alpha 2} - \omega_{\alpha 1}$, and $\Delta\omega_\beta = \omega_{\beta 2} - \omega_{\beta 1}$. Eq. (9) shows that the separation between two peaks is increased by $\gamma\Delta\omega_\beta$ with this method.

For two pairs of peaks at $\omega_{\alpha 1}$, $\omega_{\beta 1}$, $\omega_{\alpha 2}$ and $\omega_{\beta 2}$, if $\omega_{\alpha 2}$ is overlapped with $\omega_{\alpha 1}$ while $\omega_{\beta 2}$ and $\omega_{\beta 1}$ are not overlapped, $\Delta\omega_\alpha$ is very small, but $\Delta\omega_\beta$ is relatively

large. In this case, a small value of γ is sufficient to create a big Δ_γ to remove the overlapping from the spectra according to Eq. (9).

If both $\Delta\omega_\beta$ and $\Delta\omega_\alpha$ are very small, i.e., $\omega_{\alpha 1} \approx \omega_{\alpha 2}$ and $\omega_{\beta 1} \approx \omega_{\beta 2}$. It would appear difficult to separate the overlapped peaks with a small value of γ. It can be easily seen that $\omega_{\alpha 1} + \omega_{\beta 1} \approx \omega_{\alpha 2} + \omega_{\beta 2}$ in this case, and thus $\Delta\omega_\beta = -\Delta\omega_\alpha$. Substituting this last equality into Eq. (9), we obtain

$$\Delta_\gamma = |1 - \gamma| \Delta_0 \ . \tag{10}$$

This means that the separation can be increased by a factor of $|1 - \gamma|$. It can be shown that Eq. (10) is also valid for 2D ESEEM spectra. Eq. (10) indicates that a negative increment ratio γ is more effective than the corresponding positive ratio γ in increasing the separation between two overlapped cross peaks.

To compare a MIF-ESEEM spectrum with its BF-ESEEM spectrum, the same data points should be utilised. Two choices are available to do so. Firstly, as discussed in [7, 8], both the BF- and MIF-ESEEM experiments are performed with the same increment time for acquisition, e.g., $(\Delta t_1)_{BF} = (\Delta t_1)_{MIF}$ and the linewidths are the same for those two kinds of spectra. Since the separations of peaks are increased with the MIF-ESEEM scheme, the spectral resolution is enhanced. Secondly, the increment for acquisition of the BF-ESEEM experiment is $(1 + |\gamma|)$ times that of the MIF-ESEEM experiment, e.g., $(\Delta t_1)_{BF} = (\Delta t_1)_{MIF} \times$ $\times(1 + |\gamma|)$. As a result, the same time range, $(\Delta t_1)_{MIF}(1 + |\gamma|)n$ in which n is the data points, is used for these two types of ESEEM experiments. In this case, the acquisition time for the BF-ESEEM experiments is $(\Delta t_1)_{MIF}(1 + |\gamma|)n$, while that for the MIF-ESEEM experiment is $(\Delta t_1)_{MIF}$. Therefore, the linewidth becomes broadened with the MIF-ESEEM scheme. However, the increase of the peak separations overwhelms this broadening, and thus the resolution can still be enhanced.

3. Experimental

The experiments were carried out using the six-pulse sequence (see Fig. 1) [5]. All experiments were performed on an X-band (9–10 GHz) pulsed EPR spectrometer (Bruker ESP380E). The maximum power output of the microwave amplifier (about 1 kW) was used. Pulse lengths for $\pi/2$ pulses and π pulses were nominally 8 ns and 16 ns, respectively. In all of the experiments, $\tau_1 = 32$ ns and $\tau_2 = 160$ ns were chosen, and 256×256 points were recorded. The new 2D MIF-ESEEM spectrum was obtained using $(\Delta t_1')_{MIF} = (\Delta t_2')_{MIF} =$ $= 16$ ns, $\gamma = -2$, and $t_{10} = t_{20} = 8432$ ns. To be specific, one dimension is acquired with an increment of 16 ns in t_1 and -32 ns in t_2, whilst the other is obtained with an increment of -32 ns in t_1 and 16 ns in t_2. Two conventional 2D BF-ESEEM spectrum were measured using $t_{10} = t_{20} = 240$ ns. One was acquired with increments $(\Delta t_1')_{BF} = (\Delta t_2')_{BF} = 48$ ns, and $\gamma = 0$. In this case,

the time range used in both of the BF- and MIF-ESEEM experiments are 256×48 ns = 256×(16 + 24) ns = 12.288 μs. The other BF-ESEEM spectrum was measured with $(\Delta t_1')_{BF} = (\Delta t_2')_{BF} = 16$ ns, and thus the same increments are used in both the BF- and MIF-ESEEM experiments in this case. A four-step phase-cycling scheme for the six-pulse ESEEM measurements [5] was adopted to suppress unwanted spin echoes.

A single crystal of γ-irradiated malonic acid with a Dose of 10 kGy was used to demonstrate the advantages of this new spectroscopy. The magnetic field was set on one of the hyperfine EPR lines where $B_0 = 342.8$ mT, and the angle between the external magnetic field and the [001] axis of the sample is 22° [10].

4. Results and Discussion

The 2D MIF-ESEEM spectrum detected with $\gamma = -2$ of the irradiated single crystal of malonic acid is presented in Fig. 2. For the sake of comparison, its conventional 2D BF-ESEEM spectrum are shown in Figs. 3 and 4. The advantage of new 2D ESEEM spectroscopy is apparent as the overlapped peaks in Figs. 3 and 4 are well-separated in Fig. 2.

Figures 3 and 4 were acquired with increments 48 and 16 ns, respectively, so Fig. 3 has a higher digital resolution than Fig. 4. Consequently, two pairs of

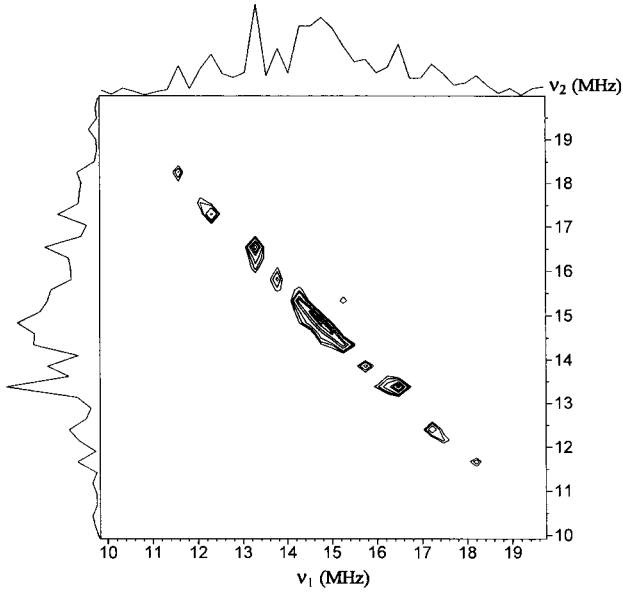

Fig. 2. A 2D ^{1}H MIF-ESEEM spectrum with $\gamma = -2$ of the γ-irradiated single crystal of malonic acid, $\Delta t_1' = \Delta t_2' = 16$ ns. The magnetic field was set on one of the hyperfine EPR lines where $B_0 = 342.8$ mT, and the angle between the magnetic field and the [001] axis of the sample is 22°. $T = 300$ K.

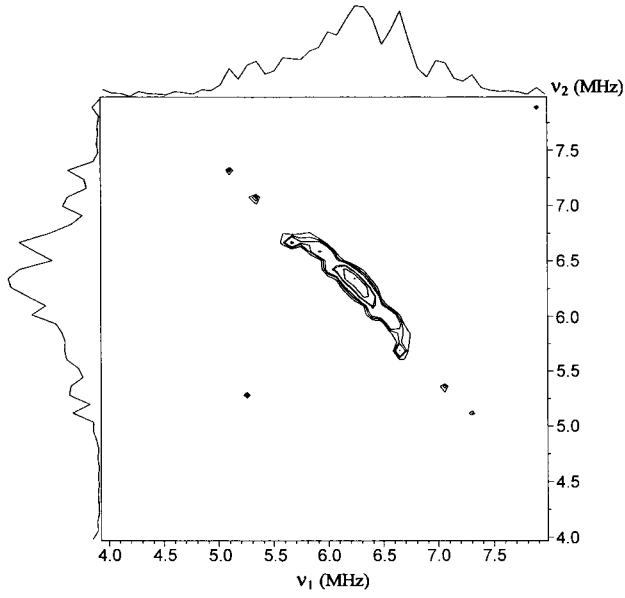

Fig. 3. A 2D ^{1}H BF-ESEEM spectrum of the same sample as in Fig. 2, $\Delta t_1' = \Delta t_2' = 48$ ns. The magnetic field was set on one of the hyperfine EPR lines where $B_0 = 342.8$ mT, and the angle between the magnetic field and the [001] axis of the sample is 22°. $T = 300$ K.

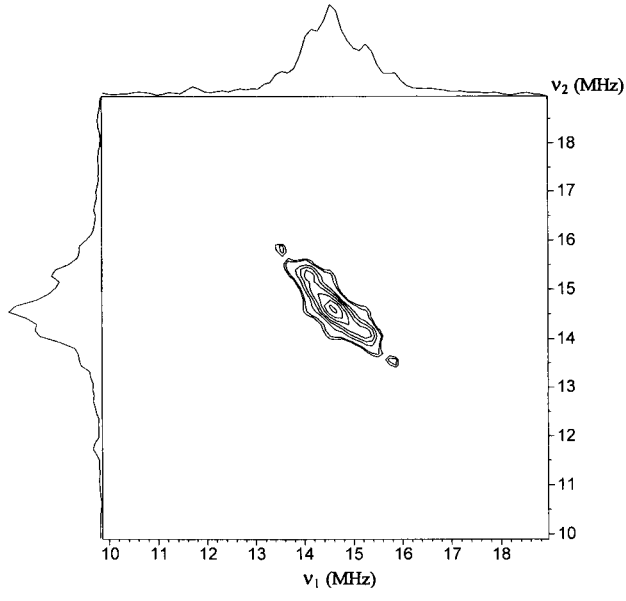

Fig. 4. A 2D ^{1}H BF-ESEEM spectrum of the same sample as in Fig. 2, $\Delta t_1' = \Delta t_2' = 16$ ns. The magnetic field was set on one of the hyperfine EPR lines where $B_0 = 342.8$ mT, and the angle between the magnetic field and the [001] axis of the sample is 22°. $T = 300$ K.

cross peaks and one diagonal peak can be seen in Fig. 3, while only one pair of cross peaks at (13.52, 15.80) and one diagonal peak appear in Fig. 4.

It should be noticed that the sampling theorem is violated in the BF-ESEEM spectrum Fig. 3. For the 2D BF-ESEEM experiment, the dwell times $\Delta t_1' = \Delta t_2' = = 48$ ns, and therefore the Nyquist frequency $\nu^N = 1/(2\Delta t_1) = 1/(2\Delta t_2) = 10.4$ MHz [11]. Since the modulation frequencies exceed this Nyquist frequency, the folding appears in Fig. 3. In our case, the relation between the real modulation frequency ν^r and the apparent frequency ν^a is

$$\nu^r = 2\nu^N - \nu^a \ . \tag{11}$$

Notice that the separations in Fig. 2 are three times large as that seen in Fig. 3, which agrees with the theoretical prediction based on Eq. (10). Although the peaks in Fig. 2 become broad they are overwhelmed by the increase in the separations between peaks. Therefore, the overlapping in the BF-ESEEM spectrum is removed with this newly-proposed method.

The basic-frequencies can be determined from Fig. 2 according to Eq. (7), and the results are listed in Table 1. Incidentally, the basic-frequencies obtained from Fig. 2 are slightly different from those calculated from Fig. 3 if $\gamma = -2$ is assumed for Fig. 2. This might be due to instrumental limitations. The increment ratio is not exactly equal to -2 for Fig. 2. In fact, by assuming $\gamma = -2.016$, the difference is removed.

It should be pointed out that the presumption for using this MIF-ESEEM spectroscopy is that the correlation between nuclear transition frequencies is already known, because basic-frequencies are determined according to Eq. (4) or Eq. (7) with the knowledge of the correlation. The new ESEEM method is aimed at line-shifting, which in turn confirms the correlations. For the systems with $I \geq 1$ or $S \geq 1$, one frequency may be correlated with two or more than two frequencies in a spectrum. The MIF-ESEEM spectra become complicated since one

Table 1. Positions of cross peaks (in MHz) in Figs. 2 and 3.

Pair	Fig. 2 (MIF)	Basic-frequencies (Calculated)[1]		Fig. 3 (BF)	Basic-frequencies (Calculated)[2]
		$\gamma = -2.016$	$\gamma = -2$		
1	18.27, 11.51	15.77, 13.53	16.02, 13.76	7.31, 5.07	15.76, 13.52
2	17.42, 12.30	15.45, 13.74	15.38, 13.34	7.08, 5.35	15.49, 13.76
3[3]	16.54, 13.29	15.17, 14.10	15.46, 14.37	6.66, 5.66	15.18, 14.18
4[3]	15.81, 13.78	14.85, 14.18	15.13, 14.46	6.58, 5.91	14.92, 14.27
5[3]	14.77, 14.77	14.49, 14.49	14.77, 14.77	6.30, 6.30	14.50, 14.50

[1] The values are obtained from Fig. 2 according to Eq. (7).
[2] The values are calculated from Fig. 3 according to Eq. (11) where $\nu^N = 10.4$ MHz.
[3] Overlapped cross peaks.

basic-frequency in a BF-ESEEM spectrum corresponds to two or more frequencies in its corresponding MIF-ESEEM spectrum. Eqs. (4) and (7) still can be used to determine basic frequencies, but it becomes complicated because of the presence of many peaks. Fortunately, for some systems with $S \geq 1$ or $I \geq 1$, one frequency is only correlated with another frequency in a spectrum, while other frequencies are absent or extremely weak. As a result, it is very easy to determine the basic frequencies using Eq. (4) or Eq. (7) just as for systems with $S = 1/2$ and $I = 1/2$.

In conclusion, the MIF-ESEEM spectroscopy is evaluated, and compared with the conventional ESEEM spectroscopy. The overlapped peaks in the conventional spectra can be separated effectively with this method. In essence, this newly-proposed ESEEM is directly based on novel signal-acquisition schemes in the time-domain, and is expected to play an important role in determining hyperfine interactions.

Acknowledgements

RS acknowledges financial support from the Australia International Development Assistance Bureau (AIDAB). Dr. Y. C. Zhong was financially supported by the Australia Research Council (A69331127 and A69531657).

References

[1] Schweiger A. in: Modern Pulsed and Continuous-Wave Electron Spin Resonance (Kevan L., Bowman M.K., eds.). New York: Wiley 1990; Dikanov S.A., Tsvetkov Y.D.: Electron Spin Echo Envelope Modulation (ESEEM) Spectroscopy. Boca Raton: CRC Press 1992.
[2] Mims W.B.: Phys. Rev. **B5**, 2409 (1972)
[3] Gemperle C., Schweiger A., Ernst R.R.: Chem. Phys. Lett. **178**, 565 (1991)
[4] Höfer P., Grupp A., Nebenführ H., Mehring M.: Chem. Phys. Lett. **132**, 279 (1986)
[5] Song R., Zhong Y.C., Noble C.J., Pilbrow J.R., Hutton D.R.: Chem. Phys. Lett. **237**, 86 (1995)
[6] de Beer R., van Ormondt D. in: Advanced EPR (Hoff A.J., ed.), pp. 135–176. Amsterdam: Elsevier 1989; Schweiger A.: Angew. Chem. Int. Ed. Engl. **30**, 256 (1991)
[7] Song R., Zhong Y.C., Noble C.J., Pilbrow J.R., Hutton D.R.: Chem. Phys. Lett. **243**, 324 (1995)
[8] Song R., Zhong Y.C., Noble C.J., Pilbrow J.R., Hutton D.R.: J. Magn. Reson. **A117**, 320 (1995)
[9] Gemperle C., Aebli G., Schweiger A., Ernst K.R.: J. Magn. Reson. **88**, 241 (1990)
[10] Goedkoop J.A., MacGillavry C.H.: Acta Cryst. **10**, 125 (1957)
[11] Ernst R.R., Bodenhausen G., Wokaun A.: Principles of Nuclear Magnetic Resonance in One and Two Dimensions, p. 337. Oxford: Clarendon Press 1987.

Author's address: Dr. Ruitian Song, Department of Physics, Monash University, Clayton, Victoria 3168, Australia